Astron. Astrophys. 322, 242–255 (1997)

ASTRONOMY AND ASTROPHYSICS

Magnetic pumping in the cataclysmic variable AE Aquarii

J. Kuijpers[1,2,3], **L. Fletcher**[⋆1,2], **M. Abada-Simon**[1,2], **K.D. Horne**[4], **M.A. Raadu**[5], **G.Ramsay**[1,2], **and D. Steeghs**[1,2,4]

[1] Sterrekundig Instituut, Universiteit Utrecht, Postbus 80 000, 3508 TA Utrecht, The Netherlands
[2] CHEAF (Centrum voor Hoge Energie Astrofysica), Postbus 41882, 1009 DB Amsterdam
[3] Dep. of Experimental High Energy Physics, University of Nijmegen, Toernooiveld 1, 6525 ED Nijmegen
[4] School of Physics and Astronomy, The University, St. Andrews, Fife KY16 9SS, Scotland, UK
[5] Division of Plasma Physics, Alfvén Laboratory, The Royal Institute of Technology, S-10044 Stockholm, Sweden

Received 10 June 1996 / Accepted 12 November 1996

Abstract. We propose that the radio outbursts of the cataclysmic variable AE Aqr are caused by eruptions of bubbles of fast particles from a magnetosphere surrounding the white dwarf. We investigate the acceleration process of magnetic pumping in the magnetosphere which is periodically driven both by the relative motion with the companion and with the infalling spray of gas at the spin frequency of the white dwarf. As the accretion rate is relatively low, the conversion of spin energy into acceleration (rather than heating) of electrons and protons can be efficient. The accelerated particles are trapped in the white dwarf magnetosphere until their total energy content becomes comparable to that of the trapping magnetic field structure and a MHD instability sets in. Synchrotron radiation is emitted in the expelled expanding plasmoid at radio and down to millimetric wavelengths. We find that there is sufficient energy transferred from the rotation energy of the rapidly-spinning white dwarf to fast particles by magnetic pumping to explain quiescent and flaring radio emissions.

Key words: acceleration of particles – magnetic fields – turbulence – cataclysmic variables – stars: individual: AE Aqr – radio continuum: stars

1. Introduction

Cataclysmic variables (CVs) are binary systems in which matter flows from a Roche-lobe filling dwarf secondary star onto a white dwarf primary. The CV AE Aqr contains one of the most rapidly spinning white dwarfs known (P_{wd} = 33 sec) and is a member of the Intermediate Polar (IP) sub- class of CVs. (For reference we give the most pertinent system parameters of AE Aqr in Table 1).

⋆ Present affiliation: ESA Space Science Dep., ESTEC, Postbus 299, 2200 AG Noordwijk

Table 1. Some of the most important system parameters of AE Aqr (most of which are taken from Welsh et al. 1994).

Period of White Dwarf ($P_{wd} = 2\pi/\omega_{wd}$)	33.0767 sec
Binary orbital period ($P_{bin} = 2\pi/\Omega_{binary}$)	9.8797 hr
M_1	$0.89 M_\odot \pm 0.23$
M_2	$0.57 M_\odot \pm 0.15$
Secondary spectral type	K3–5V
Inclination i	$55^\circ \pm 7$

The magnetic field strength of the white dwarf in IP's is not sufficient to synchronise the spin period of the white dwarf with the binary orbital period, but prevents or disrupts the formation of an accretion disk which is usually present in CVs (see Patterson 1994 for a recent review). In Polars (or AM Her stars), the white dwarf has a sufficiently strong magnetic field to prevent the formation of an accretion disk and the accretion flow impacts directly onto the white dwarf (see Cropper 1990 for a review). However, a direct measurement of the magnetic field strength of AE Aqr has yet to be made. The most common method of determining this parameter in Magnetic CVs is from polarisation measurements. Measurements by Stockman et al. (1992) gave an upper limit to the circular polarisation of 0.06% indicating B <500 T. Other more indirect estimates of the field strength include B=1–10 T and 10–100 T (Lamb & Patterson 1983 and Lamb 1988 respectively) from the spin-down and pulsing behaviour of the white dwarf.

Although the magnetic field strength of AE Aqr is uncertain, there is evidence to suggest that there is no accretion disk at the present epoch, and that very little of the material leaving the secondary star is actually accreted onto the surface of the white dwarf. The observed emission lines are not double peaked, and a Doppler tomograph (Wynn et al. 1996) shows no signature of the expected Keplerian flow. This would suggest that the accretion is largely stream-like, or possibly blob-like. Wynn et al. (1995) simulate the accretion flow in AE Aqr and find that the vast bulk of material is ejected from the binary system altogether. This is also consistent with optical observations by Mouchet et al.

(1995) which show no evidence for the presence of an accretion disc.

AE Aqr is observed to emit at radio wavelengths with a quiescent and a flaring component. The generation mechanism probably is synchrotron emission from relativistic electrons gyrating in magnetic fields. The integrated quiescent radio power at a distance of 84 pc (Bailey 1981) is $2.8 \cdot 10^{20}$ W, that in flares $1.4 \cdot 10^{21}$ W. The X-ray emission is $\sim 10^{25}$ W ($L/L_{Edd} = 0.48 \cdot 10^{-6}$) implying an accretion rate of at most $8.5 \cdot 10^{11}$ kg s^{-1} $= 1.3 \cdot 10^{-11}$ $M_\odot$/yr (if all luminosity is from accretion, Eracleous et al. 1991, Reinsch et al. 1995). This emission is smaller by more than an order of magnitude than the spin-down luminosity of the white dwarf ($6 \cdot 10^{26}$ W; De Jager 1994). The spin-down energy is much larger than the (total observed) quiescent accretion luminosity plus the energy released in typical UV flares (Horne & Eracleous 1995). There is therefore a reservoir of energy which might be tapped to accelerate to high energy the particles thought to be the source of quiescent and flaring radio emission.

Bastian et al. (1988) and Abada-Simon et al. (1993) reported radio flares on timescales ranging from a few minutes to several hours. They interpreted these flares as the superposition of synchotron-emitting plasma clouds. Observations of AE Aqr were extended down to sub-mm wavelengths by Abada-Simon et al. (1995a). Typically the radio power is 10^{21} W during one hour for a big flare, and a total radio energy of a few times 10^{24} Joules (10^{25} J for the largest flare observed). The optical and radio flare events are not correlated and further, unusual dips were seen in the radio (Abada-Simon et al. 1995b). From VLBI a source expansion up to $4a$ (a is the binary separation) has been inferred at a speed 0.01 c (A.E. Neill 1995 private communication, De Jager & Meintjes 1993). Although Bastian et al. (1988) proposed a model in which energetic particles were the direct cause of these flares, they did not attempt to explain what the source of these energetic particles was. Under the synchrotron hypothesis a total energy of $W \sim 4 \cdot 10^{24}$ J is required in $5 \cdot 10^{35}$ energetic electrons with Lorentz factors of $\gamma \sim 90$ distributed over a source of extent $3 \cdot 10^8$ m with an ambient magnetic field of 0.005 T. In the present work we attempt to explain the origin of these fast particles. We will address the following questions:

- What is the power in MHD disturbances? (§2)
- Is magnetic pumping a suitable candidate for the particle acceleration required to power the synchrotron emission? (§3,4,5,6)
- What causes the radio emission to be produced in flares rather than more steadily? (§6)
- What other acceleration processes are relevant to AE Aqr? (§7)
- Why do radio outbursts such as observed on AE Aqr occur only in 4 CVs and in only a small fraction of X-ray binaries (Nelson & Spencer 1988, Hjellming & Penninx 1991, Kuijpers 1989)? (§7)

In Sect. 2 we first consider how effectively magnetic disturbances are created in the magnetised white dwarf companion system. In Sect. 3 we work out which adiabatic invariants exist in AE Aqr and discuss their relevance to particle acceleration. In Sect. 4 we specifically study acceleration by magnetic pumping, and in Sect. 5 the limiting particle energies when account is taken of various losses. In Sect. 6 we model the radio emission. In Sect. 7 we discuss the initial particle source, other potentially significant acceleration processes, and the relation of AE Aqr to other magnetised binaries. Finally Sect. 8 sums up the results of the present paper.

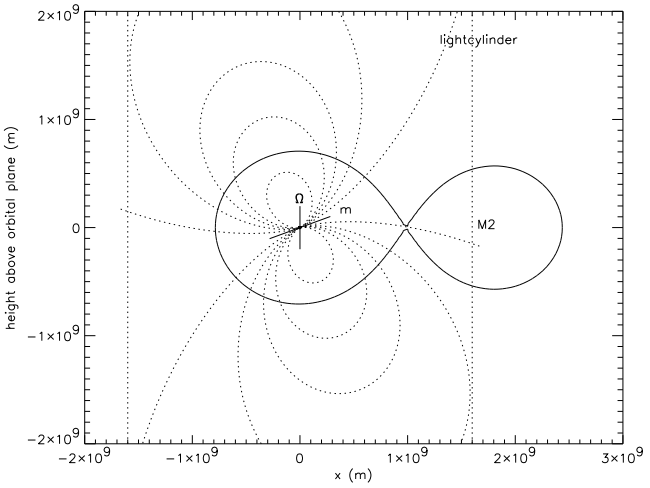

Fig. 1. The Binary System AE Aquarii. Shown are the system Roche Lobes, the orientation of the spin axis (here vertical), the position of the light cylinder, and the position of the magnetic dipole axis as it passes the plain of the drawing. Also shown are some of the unperturbed dipolar field lines including the last closed field lines and the two field lines which would pass through the inner Lagrangian point at the epoch represented and, respectively, half a spin period later.

2. Magnetic powering

The geometry of the system is sketched in Fig. 1 for the orientation of the magnetic dipole inferred from UV observations (Welsh et al. 1993, Eracleous et al. 1994). The light cylinder at a radius $r_{lc} = c/\omega_{wd} = 1.58 \cdot 10^9$ m reaches out past the inner Lagrangian point but does not contain the secondary star entirely. The figure also shows a number of unperturbed dipolar field lines, including the field lines through the inner Lagrangian point. The cones of 'open' – reaching outside the light cylinder – field lines on opposite hemispheres encompass practically the entire set of (unperturbed) field lines going through the inner Lagrangian point during a rotation period of the white dwarf. These polar caps of open field lines at the white dwarf surface are small: for a dipole with obliquity 70° the half-width in the azimuthal direction is $\theta_{pc} = (\omega_{wd} R_{wd}/c)^{0.5} = 4.6^\circ r_7^{0.5}$ while in the meridional plane it extends 1.9° and 3.4° away from the magnetic pole for a white dwarf radius $R_{wd} = 10^7\ r_7$ m.

Since the rotation of the white dwarf is fast compared to the orbital period ($P_{wd} = 33.0767$ s $\ll P_{bin} = 9.88$ hours) the white dwarf magnetosphere is strongly perturbed by the relative motion of the companion. Moreover, any gas streaming from

the inner Lagrangian point onto the white dwarf will similarly perturb the fast moving magnetosphere, until the gas reaches its Alfvén radius r_A (defined loosely by equating the ram pressure ρv^2, v is the relative speed between gas and magnetosphere, to the ambient stellar magnetic pressure $B^2(2\mu_0)^{-1}$). Thereafter, depending on the location of the Alfvén radius with respect to the radius of corotation

$$r_{co} = (GM_1)^{1/3}\omega_{wd}^{-2/3} = 1.49 \cdot 10^7 (M_1/0.89\ \mathrm{M}_\odot)^{1/3}\ \mathrm{m}, \quad (1)$$

the gas will either be propelled away (when $r_A > r_{co}$) or, when the reverse inequality is satisfied, be caught by the field and fall onto the white dwarf.

2.1. Power radiated in MHD waves

The power radiated in MHD (mainly Alfvén) waves by a good conductor of spherical shape (cross-section A) moving at subalfvénic speed v through an ambient magnetic field of strength B can be obtained from Barnett & Olbert (1986) under a number of assumptions

$$P_A = 7.11 A \frac{B^2}{2\mu_0} v \frac{v}{v_A}, \quad (2)$$

where v_A is the Alfvén speed in the ambient medium. It is assumed that the radius of the sphere is much larger than an effective gyroradius v/ω_{ci0} ($\omega_{ci0} = eB/m_i$ is the proton Larmor frequency), the cold plasma approximation is used (valid if $v^2 \gg c_s^2$), the ambient plasma is dense enough ($\omega_{pe}^2 > \omega_{ce0}^2$, where $\omega_{pe} = (ne^2/m_e\epsilon_0)^{0.5}$ is the electron plasma density, $\omega_{ce0} = eB/m_e$ is the electron Larmor frequency), and finally, the Alfvén crossing time over the dimension of the sphere is much less than the Ohmic diffusion time. In our case all but one of these assumptions are correct: the ratio ω_{pe}/ω_{ce0} is probably much less than unity for the magnetosphere of AE Aqr. However we do not expect that this changes the above result significantly as long as one uses the correct relativistic Alfvén speed given by $v_A^{-2} = c^{-2} + B^{-2}\mu_0\rho$.

The radiated power by an antenna is known to be very sensitive to matching of impedances between antenna and the external medium. The detailed shape of the emitter (Lüttgen & Neubauer 1994) and the far-field boundary conditions are therefore crucial in these calculations. For instance, if the magnetosphere acts as a cavity, standing waves can be set up and the power radiated by an antenna then depends on the dissipation of the waves in the cavity. If the antenna were placed in a homogeneous medium the radiated power would not necessarily depend on the wave dissipation. Further, if the plasma is not cold and if moreover the conductor is injecting plasma into the magnetosphere, such as is the case for Io moving in Jupiter's magnetosphere, the slow mode can also be excited and magnetic field perturbations arise not only along so-called Alfvén wings but also in the wake of the satellite (Kopp 1996). This case may be particularly relevant for AE Aqr as the infalling gas blobs are expected to become ablated by the rotating magnetosphere.

Finally we mention another process for radiation of MHD waves by infalling gas. Scheurwater & Kuijpers (1988) calculated the efficiency of MHD wave excitation from a localized pressure pulse, generated by a plasma sphere falling along the stellar magnetic field and hitting the stellar surface at subalfvénic speed. Of the total infall energy a fraction $0.14(n_c/n)(v/v_A)^3$ is radiated into Alfvén waves and a fraction $1.8(n_c/n)(v/v_A)^7$ into fast magnetosonic waves, where n_c is the particle density inside the cloud and n the ambient density above the surface. This demonstrates that the matter which finally accretes (with an accretion energy up to 10^{25} W) onto the surface of the white dwarf is an efficient source of MHD waves.

Let us now compare the power radiated in MHD waves by the companion with that radiated by infalling gas, applying the simple estimate (2) with a coefficient one.

2.2. Power radiated by the companion

Since the companion is near the light cylinder, its relative motion through the magnetosphere of the white dwarf is probably superalfvénic and it will possess a bow shock. We can then estimate the MHD power generated in the stellar wake by putting $v = v_A$ in the previous equations and writing $v = (\omega_{wd} - \Omega_{bin})r \approx \omega_{wd} r$:

$$P_c \approx R_c^2 \omega_{wd} a (R_{wd}/a)^6 B_{wd}^2 (2\mu_0)^{-1} = 1.96 \cdot 10^{22} B_2^2\ \mathrm{W}, \quad (3)$$

where we have taken a radius for the companion $R_c = 7 \cdot 10^8$ m, a distance from the white dwarf $a = 1.8 \cdot 10^9$ m and a field strength $B_{wd} = 100 B_2$ T at the surface pole of the white dwarf with radius $R_{wd} = 10^7$ m.

2.3. Power radiated by infalling gas

To estimate the power radiated in MHD waves by infalling gas we use an accretion rate $\dot{M} \sim 5 \cdot 10^{11}$ kg/s based on the quiescent X-ray luminosity. For simplicity we assume that a steady flow of gas escapes at a rate $\dot{M}$ from the inner Lagrangian point at a sound speed $c_s = 8.4$ km/s ($T = 10,500$ K) through a nozzle with cross-section H^2 and $H = 100$ km (much smaller than the scale height near the inner Lagrangian point, see below). Further, we assume that the gas stream remains isothermal and keeps the same cross-section and that its velocity quickly reaches the free-fall speed in the gravitational field of the white dwarf $v_f = 486\ r_9^{-0.5}$ km/s ($r_9 \equiv r/(10^9\ \mathrm{m})$). We take the cross-section to be constant until the stream reaches the pressure balance radius, defined by the distance at which the gas pressure becomes equal to the ambient stellar field pressure. For a dipolar magnetic field dependence we find a pressure balance radius,

$$r_{p7} = 21.5 B_2^{4/13} (c_s/8.4\ \mathrm{km/s})^{-4/13} (\dot{M}/5.38 \cdot 10^{11}\ \mathrm{kg/s})^{-2/13} (H/100\ \mathrm{km})^{4/13}. \quad (4)$$

Inside the pressure balance radius we assume that infall is again steady at the same rate, at the same temperature, and at the free-fall speed, now however with the cross-section determined

by balance between the gas pressure and the ambient magnetic field pressure. Assuming the relative transverse speed between gas stream and magnetosphere to be supra-Alfvénic everywhere we arrive at the following estimate for the power radiated in MHD waves by a steady stream with a transverse extent $h(r)$ extending from the Lagrangian point at a distance 10^9 m down to the Alfvén radius (or the white dwarf radius at 10^7 m, whichever is larger)

$$\begin{aligned} P_a &= \int B_{wd}^2(2\mu_0)^{-1}(r/R_{wd})^{-6}\omega_{wd} r h(r) dr \\ &= \frac{B_{wd}^2}{2\mu_0}\omega_{wd}R_{wd}^2[\frac{4c_s(2\mu_0\dot{M})^{0.5}R_{wd}^{0.25}}{3B_{wd}(2GM_1)^{0.25}}(\frac{r}{R_{wd}})^{-0.75}|_{r(h=H)}^{R_{wd}} \\ &+ \frac{H}{4}(\frac{r}{R_{wd}})^{-4}|_{10^9\mathrm{m}}^{r(h=H)}] \approx 3.60\cdot 10^{24}B_2 \text{ W}. \end{aligned} \quad (5)$$

Under our assumptions the stream becomes compressed inside $r(h = H) = 21.5 \cdot 10^7$ m and extends down to the white dwarf (because of the assumptions of isothermality and pressure equilibrium, the stream is very dense and never reaches its Alfvén radius ($\rho v_f^2 \gg \rho c_s^2 \approx B^2(2\mu_0)^{-1}$), which in this case simply reduces to $r = c_s/\omega_{wd} = 4.4 \cdot 10^4$ m $< R_{wd}$). Note that the *spin-down luminosity* in MHD waves (estimate (5)) can be comparable to the quiescent *gravitational* X-ray luminosity which we used to estimate the mass loss. Of course for consistency it is required that the MHD power is not ultimately converted into X-rays.

Note that we have assumed a very small thickness of the gas stream, $H = 100$ km, in comparison to the scale height at the inner Lagrangian point, $H_L \sim c_s P_{bin}(2\pi)^{-1} \sim 4.8 \cdot 10^4$ km (Frank et al. 1992). As the efficiency of MHD wave excitation increases with the transverse extent of the gas stream, a small value of the thickness leads to a conservative estimate. In reality, the gas blobs will first fall freely towards the white dwarf. In the comoving frame the gas will expand along the equatorial plane at the speed of sound (which will of course decrease quickly due to adiabatic expansion). Transverse to the orbital plane the gas also expands as long as the gravitational acceleration is large compared to the centrifugal acceleration. When the latter increases, the gas tries to reach pressure equilibrium with the remaining effective field of gravity but will not succeed completely as it needs at least a free-fall or Keplerian time to do this. As a rough approximation for the transverse thickness we could therefore take $H = rc_s/v_{Kep}(r) \sim 515 r_8^{1.5}$ km, as long as the ambient magnetic field pressure remains much smaller than the gas pressure (that is outside the pressure balance distance). As can be seen from (5) an increased transverse extent H causes an increase of radiated MHD power. Because of the unknown amount of equatorial spreading we shall use the conservative estimate (5). In principle the MHD power could increase by over two orders of magnitude, up to the observed spin-down luminosity $6 \cdot 10^{26}$ W.

We conclude that the fast spinning white dwarf emits a *spin-down* luminosity in the form of MHD waves with a lower limit of $P_c \sim 2 \cdot 10^{22} B_2^2$ W determined by the presence of the non-corotating companion, and a value of $4 \cdot 10^{24} B_2$ W if mass transfer takes place at a rate $5.4 \cdot 10^{11}$ kg/s provided the local rotation speed is (super)Alfvénic. In a realistic magnetosphere the radiated waves will not be purely Alfvénic but have a compressive component because of the inhomogeneity and line-tying of the fields.

Is this sufficient in principle to power the observed radio emission? The quiescent radio power is $\sim 2.8 \cdot 10^{20}$ W (Abada-Simon et al. 1995b), and an order of magnitude larger during flaring. The net conversion efficiency of MHD waves into radio emission should then on average be 10^{-4} up to 10^{-2}. In the next section we examine the properties of particle orbits in the present system and how violation of particular adiabatic invariants can cause stochastic acceleration.

3. Invariants and acceleration

The motion of a particle in a slowly time- and space-varying magnetic field in the absence of collisions can be characterized by a drift motion of the so-called center of gyration around which the particle performs its gyration orbit. For a particle of charge q, rest mass m and Lorentz factor γ, the perpendicular drift of the gyrocentre under the influence of a force $\boldsymbol{F}$ (Alfvén & Fälthammar 1963) is given by

$$\boldsymbol{v}_d = \frac{\boldsymbol{F}\times\boldsymbol{B}}{qB^2}. \quad (6)$$

The frequency of gyration of a charged particle (charge q_j, rest mass m_j) with perpendicular velocity component $v_\perp$ ($\beta_\perp = v_\perp/c$) is given by its cyclotron frequency

$$\omega_{cj} = \frac{|q_j|B}{\gamma m_j} = 1.76\cdot 10^{11}\frac{B}{\gamma}\frac{m_e}{m_j} \text{ rad/s}, \quad (7)$$

and its cyclotron radius by

$$r_{cj} = \frac{v_\perp}{\omega_{cj}} = 1.7\cdot 10^{-3}\frac{\gamma\beta_\perp}{B}\frac{m_j}{m_e} \text{ m}. \quad (8)$$

Up to first order in ω/ω_c and in kr_c, where ω is the angular frequency, and $\boldsymbol{k}$ the wave vector of the field perturbations, the total gyrocentre speed (in the case of a particle in the WD magnetosphere) is (Roederer 1970, Goldston & Rutherford 1995)

$$\begin{aligned} \boldsymbol{v}_{gc} &= v_\parallel\hat{b} + \frac{\boldsymbol{E}\times\boldsymbol{B}}{B^2} - \frac{\mu\boldsymbol{\nabla}B\times\boldsymbol{B}}{qB^2} \\ &- \frac{\gamma m v_\parallel^2[(\hat{b}\cdot\boldsymbol{\nabla})\hat{b}]\times\boldsymbol{B}}{qB^2} - \frac{m d\boldsymbol{v}_{gc}/dt\times\boldsymbol{B}}{qB^2}, \end{aligned} \quad (9)$$

where $v_\parallel$ is the particle velocity component along the magnetic field, $\hat{b} = \boldsymbol{B}/B$ is the unit vector along the magnetic field, $\boldsymbol{E}$ is the electric field, μ is the magnetic moment

$$\mu = \frac{p_\perp^2}{2\gamma m B}, \quad (10)$$

and we have assumed the drift motion to be sub-relativistic. The perpendicular drifts in Eq. (9) correspond to, respectively, the

electric field drift, the gradient drift, the curvature drift, and the inertial drift. We have left out the drift due to gravity as it is relatively unimportant for particles which have enough energy to remain in the magnetic fields surrounding the white dwarf.

In the same approximation – as long as the cyclotron frequency of the particle is much larger than the oscillation frequency of the field, and as long as the spatial scale of the field is much larger than the particle cyclotron radius –the following quantity is conserved

$$\frac{p_\perp^2}{B} = \frac{\gamma^2\beta_\perp^2 m^2 c^2}{B} = \text{const}, \tag{11}$$

which is the so-called *first adiabatic invariant*. Here $p_\perp = \gamma m v_\perp$ is the particle momentum perpendicular to the magnetic field. It is important to realize that the quantity (11) relates to individual particles following their motion as they drift across the field. Therefore the perpendicular energy changes as

$$v_\perp \frac{dp_\perp}{dt} = \mu\frac{dB}{dt} = \mu\frac{\partial B}{\partial t} + \mu(\boldsymbol{v}_{gc}\cdot\boldsymbol{\nabla})B. \tag{12}$$

Finally, the evolution of the parallel energy is governed by (Goldston & Rutherford 1995)

$$v_\parallel \frac{dp_\parallel}{dt} = \boldsymbol{v}_{gc}\cdot(q\boldsymbol{E} - \mu\boldsymbol{\nabla}B). \tag{13}$$

Note that Eqs. (12) and (13) demonstrate that the total particle energy only changes in the presence of electric fields.

Apart from the first adiabatic invariant (10), valid when the field changes slowly ($\omega/\omega_c \ll 1$ and $kr_c \ll 1$), two more invariants can be distinguished. The quantity

$$J = \oint p_\parallel dl \tag{14}$$

the *longitudinal invariant,* is conserved when the timescale of the field is much larger than the bounce time of a particle on a trapped orbit, $\omega t_b \ll 1$, where (Lyons & Williams 1984)

$$t_b = \oint \frac{dl}{v_\parallel(l)} = \frac{4R_0}{v} f_1(\theta_0) = 0.133\frac{R_0}{R_{wd}}\beta^{-1} f_1(\theta_0)\ \text{s}, \tag{15}$$

and the last two equalities are for a dipole field with $f_1(\theta_0) \approx 1.38 - 0.32(\sin\theta_0 + \sin^{0.5}\theta_0)$ and θ_0 is the particle pitch angle (the angle of the velocity vector to the local magnetic field direction) when it crosses the magnetic equator at a radial distance R_0 (the quantity R_0/R_{wd} is known as the magnetic shell parameter).

A third adiabatic invariant, the *flux invariant,* exists when the particle executes a bounce averaged periodic drift motion and the timescale of field changes is large compared to the bounce average drift period, $\omega t_d \ll 1$. The flux invariant is defined as the magnetic flux linked in the particle's drift averaged over the bounce motion

$$\Phi_M = \oint \boldsymbol{A}\cdot d\boldsymbol{l}, \tag{16}$$

where $\boldsymbol{A}$ is the magnetic vector potential. The bounce average drift period for a dipole field is

$$\begin{aligned} t_d &= \frac{2\pi q B_{wd} R_{wd}^2}{3mc^2}\frac{R_{wd}}{R_0}\frac{1}{\gamma\beta^2 f_2(\theta_0)} \\ &= 2.33\cdot 10^7(\gamma\beta^2 f_2(\theta_0) R_0/R_{wd})^{-1}\ \text{s}, \end{aligned} \tag{17}$$

where the last result is for a proton and $f_2(\theta_0) \approx 0.70 + 0.30\sin\theta_0$.

Clearly as in our case the dominant perturbations in the fields are at periods below 33 s the third invariant does not exist. However, both the first (11) and the second invariant (14) exist as the inequalities $1 \ll \omega_c P_{wd}/2\pi$ (see Eq. (7)) and $t_b \ll P_{wd}/2\pi$ (see Eq. (15)) are easily satisfied for fast particles as long as they can be considered collisionless.

The above arguments suggest a number of single-step (non-stochastic) acceleration processes may occur in the magnetosphere of AE Aqr. For instance the magnetic field will vary in time by a factor of a few, and cause a similar increase in particle energy on account of (11). A more interesting possibility is when a particle somehow drifts from the companion to the surface of the white dwarf. Two magnetic shells of the rotating (dipolar) magnetosphere have an electric potential difference of magnitude

$$\begin{aligned} \Delta\Phi &= \int[(\boldsymbol{\omega}_{wd}\times\boldsymbol{r})\times\boldsymbol{B}]\cdot d\boldsymbol{l} = \frac{\omega_{wd}\Delta\Phi_M}{2\pi} \\ &= 0.5\omega_{wd}R_{wd}^2 B_{wd}\Delta(R_{wd}/R) \le 9.52\cdot 10^{14}\ \text{Volt}, \end{aligned} \tag{18}$$

where $\Delta\Phi_M$ is the magnetic flux trapped between both shells. This may lead to the production of TeV particles which have possibly been detected (Meintjes et al. 1994).

If collisions or fluctuations on a small spatio-temporal scale (either $\omega/\omega_c \ge 1$, or $kr_c \ge 1$) occur the quantities (11) and (14) are not invariants during the short-lasting interaction. The combination of the existence of invariants during part of the time combined with pitch-angle scattering causes a rich variety of stochastic particle acceleration mechanisms to appear under periodic (instead of single-step) field changes, depending on the relative ordering of the scattering timescale and the particle orbital periods (e.g. Alfvén & Fälthammar 1963, and for planetary magnetospheres, Möbius 1994). Here we will concentrate on one such process of particular importance for AE Aqr; that of magnetic pumping (sometimes termed betatron acceleration).

4. Acceleration by magnetic pumping

Magnetic pumping is one of a number of stochastic particle acceleration mechanisms (known also as Fermi-type mechanisms) whose essential property is the combination of a particle interaction with a spatial or temporal change in the magnetic field – which causes the particle energy to change – with a randomising process (Swann 1933, Fermi 1954, Alfvén 1954, Spitzer 1962). Usually a distinction is made between two kinds of magnetic pumping: *transit-time* and *'collisonal'* magnetic pumping (Stix 1992, Berger et al. 1958, Schlüter 1957). In both cases a confining magnetic field is being modulated at frequency f (assumed

to be small in comparison with the particle cyclotron frequencies) over a distance d. Transit-time pumping occurs when the bounce time of the particles is approximately equal to the modulation frequency: $f \approx d/v$. In 'collisional' pumping particles are scattered in pitch angle by an independent process, sometimes but not necessarily by particle collisions.

Here we will investigate the latter process of 'collisional' magnetic pumping for arbitrary large field modulations, now however invoking unspecified collisionless wave-particle scattering instead of collisional pitch angle scattering, so that acceleration instead of heating occurs. This complements Kulsrud & Ferrari (1971) who calculated acceleration by small-amplitude slowly-varying large-scale hydromagnetic turbulence in a uniform background field in the presence of pitch-angle scattering. It also complements the 'gyro-relaxation' by Schlüter (1957) and the collisonal magnetic pumping by Berger et al. (1958), both for a one-temperature gas and small amplitude variations of a uniform background field. In the Discussion at the end we briefly discuss the effects of transit-time pumping.

Although particles may gain or lose energy in the interaction, randomisation ensures that on average an increase occurs. In the case of magnetic pumping, an increase in the magnitude of the magnetic field causes the particle momentum perpendicular to the magnetic field to increase, by conservation of the first adiabatic invariant $p_\perp^2/B$ (11). If there is no other process to change the particle momentum, a decrease of the field to the old value results in the particle losing exactly the amount of energy it gained. However if it can be arranged that the particle scatters, moving some of its newly gained perpendicular energy into the parallel direction, decompression of the field (which only affects the perpendicular component) leaves the particle with slightly more energy than it had to begin with. On average the increase in energy (= $\gamma - 1$ in units of the rest-mass energy mc^2) by pumping of angular frequency ω is given by

$$\dot{\gamma}_{bet,av} = \frac{\alpha\omega}{4\pi}\left(\frac{\Delta B}{B}\right)^2 \frac{1}{1+\Delta B/B}\frac{(\gamma^2-1)}{\gamma}, \tag{19}$$

where α is a small coefficient and the field varies periodically between the values B and $B + \Delta B$. The value $\dot{\gamma}_{bet,av}$ is the *average* increase in the particle population energy with time due to the magnetic pumping process; α depends primarily on the ratio of field oscillation time to pitch-angle scattering timescale.

In a few illustrative cases (e.g. Alfvén & Fälthammar 1963, Melrose 1980), α can be estimated from heuristic considerations, but we shall approach it numerically, deriving it from the evolution for the distribution function $f(\gamma, t)$ of particles undergoing pumping. From (11) the equation for individual particle trajectories in a time-varying magnetic field is

$$\frac{\dot{p}_\perp}{p_\perp} = \frac{\dot{B}}{2B}, \tag{20}$$

and in the absence of other processes the continuity equation for the distribution function $f(p_\perp, p_\parallel, t)$ (averaged over gyration phase) of many such particles is

$$\frac{\partial f(p_\perp,p_\parallel,t)}{\partial t} + \frac{1}{p_\perp}\frac{\partial}{\partial p_\perp}\left(\frac{\dot{B}p_\perp^2}{2B}f(p_\perp,p_\parallel,t)\right) = 0. \tag{21}$$

If we rewrite this equation in terms of (p, μ, t), where $\mu = \cos\theta$, θ is the pitch-angle, now including a term representing particle scattering, the distribution evolution equation becomes (correcting Kirk 1995)

$$\frac{\partial f(p,\mu,t)}{\partial t} + \frac{\dot{B}}{2B}(1-\mu^2)\left(p\frac{\partial f(p,\mu,t)}{\partial p} - \mu\frac{\partial f(p,\mu,t)}{\partial \mu}\right) + \frac{\dot{B}}{B}f(p,\mu,t) = \left(\frac{df(p,\mu,t)}{dt}\right)_{scatt} \tag{22}$$

This represents an intrinsically reversible energisation process, made irreversible by the isotropisation of the energised particles in the period between compression and re-expansion of the field. If we solve for the particle distribution function, we may fit the results to the averaged form for energy increase (19), thus identifying the coefficient α for different cases.

We solve equation (22) with a scattering term

$$\left(\frac{df}{dt}\right)_{scatt} = \frac{\partial}{\partial\mu}D_{\mu\mu}\frac{\partial f}{\partial\mu}, \tag{23}$$

where $D_{\mu\mu}$, the diffusion coefficient, is the inverse of the scattering timescale. At present we have neither energy nor pitch-angle dependence of the diffusion coefficient.

The solution of equation (22) is accomplished by means of the method of stochastic simulations (MacKinnon & Craig 1991) which has been used recently in the solution of transport equations for the case of electrons propagating in the solar corona and chromosphere (Fletcher 1995, Fletcher & Brown 1995) and of cosmic rays accelerated at shocks (Achterberg & Krülls 1992, Krülls & Achterberg 1994). The method has been described in some detail in the above references, and here we state only a few important points. It is based on the formal mathematical equivalence of a Fokker-Planck type of equation (such as (22)) with a set of stochastic differential equations describing the motion of individual particles and is similar to a Monte Carlo formulation in implementation, in that the evolution of the particle distribution function is calculated by generating many realisations of individual particle orbits, and binning the results. The difference with a conventional Monte Carlo simulation lies in the interpretation of diffusion terms. Whilst a Monte Carlo calculation simulates individual collisions, the stochastic method scales the mean free path and collision frequency in a manner which is entirely determined by the physics which appear in the transport equation (cf Achterberg & Krülls 1992), making it a very 'physical' method, as well as extremely easy to implement computationally. As the scattering is a Gaussian process, the error on each bin of the histogram is $\sqrt{N}/N$, for a bin containing N particles. In the calculations we shall impose an oscillating magnetic field on a population of test electrons in a background

of electrons and ions. The test electrons represent electrons that have been injected into, or have attached themselves onto, the magnetic field of the white dwarf.

We can consider two categories of acceleration. The first is *standing* compressional oscillations, and the second *travelling* compressional oscillations. In general both standing and travelling oscillations can be excited by the companion as well as by the infalling gas. Large oscillations are generated by the field lines opening and closing around the companion and can be expected to cause a standing wave pattern. However, the passage of a stream of smaller blobs of material through the field can also lead to standing oscillations in the inner magnetosphere if a resonance condition exists, and the spin period and the Alfvén travel time along the field lines have a rational relation. As has been demonstrated, the power in the latter can easily be 100 times that in the former. We investigate the possibility that the acceleration occurs by oscillations at the spin frequency, either as standing or as travelling magnetic compressions.

4.1. Acceleration by standing magnetic compressions.

Standing magnetic compressions are caused by the large-scale oscillations of the field as it sweeps by the companion. The field oscillation is purely transverse - there is no component of the wave vector along the field. If we restrict our considerations to the non-relativistic regime, Eq. (19) becomes

$$\dot{E} = \frac{\alpha\omega}{2\pi}\left(\frac{\Delta B}{B}\right)^2 \frac{E}{1+\Delta B/B} \tag{24}$$

which is linear in a plot of $ln(E/E_o)$ versus t, with gradient $\frac{\alpha\omega}{2\pi}\left(\frac{\Delta B}{B}\right)^2\left(1+\frac{\Delta B}{B}\right)^{-1}$, to which we can easily fit numerical results.

In Fig. 2 we plot the mean energy increase with time for 5,000 numerical particles in a few runs, demonstrating clearly the linear relationship found by the stochastic simulation. Repeating a number of times we generate Fig. 3, showing α against τ_{scatt}/τ_{osc}. Note that, although we have chosen specific values of $B, \Delta B/B$ and ω for this calculation, the values of α found are robust to changes in these parameters.

In this type of acceleration, similar to second-order Fermi acceleration, we find that a particle initially in the non-relativistic energy regime spends much of its time being accelerated to relativistic energies, thereafter the increase to ultra-relativistic energies happens very quickly.

It is evident that the efficiency of particle acceleration reaches a maximum at $\alpha \sim 0.40$ for $\tau_{scatt}/\tau_{osc} = 1$. Alfvén & Fälthammar (1963) find a value of $\alpha = 2/9$, half as large, in an idealised situation in which scatterings only occur at the precise minima and maxima of the field. This type of wave can, for $\Delta B/B \gtrsim 0.25$ accelerate particles to relativistic energies within a few thousand seconds starting from their characteristic free-fall energy down the potential well of the white dwarf. However, in a high field environment the energy loss of the particles in synchrotron emission should be included. This may result in an equilibrium between energy gain and loss by electrons, and is investigated in § 5.

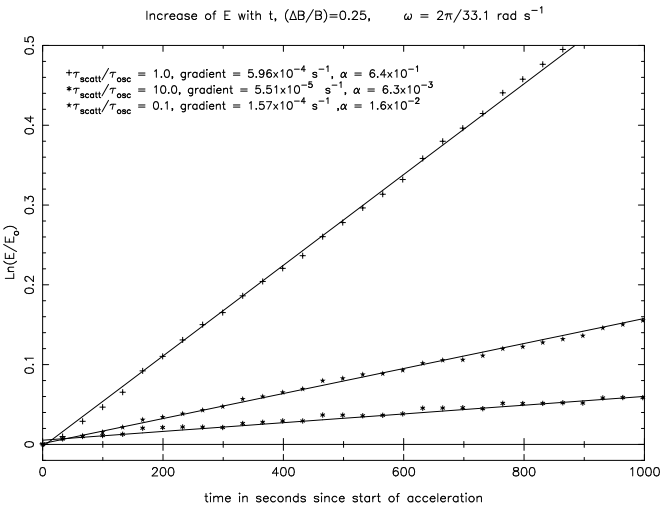

Fig. 2. The increase of energy with time by homogeneous magnetic pumping in the non-relativistic regime, for 3 values of the pitch-angle scattering to field oscillation time. The straight lines are fits to the numerical data, given by the points. α is calculated given the field parameters indicated.

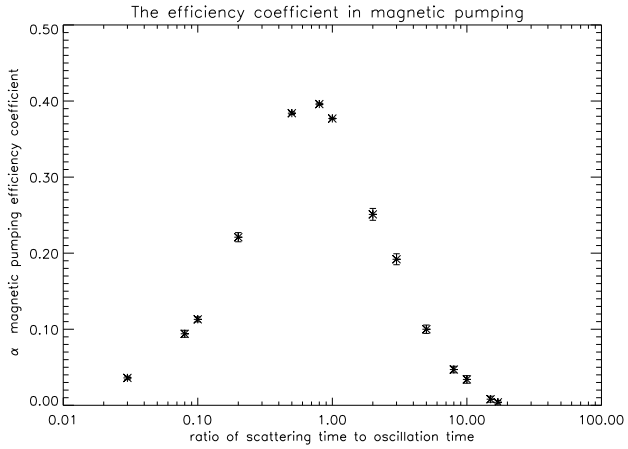

Fig. 3. The parameter α as a function of the ratio of pitch-angle scattering time to field oscillation time.

4.2. Acceleration by travelling magnetic disturbances.

Here we look at travelling waves, which are typically those caused by the infall of blobs of material. We envisage that a train of Alfvén and compressional waves is set up in the ambient field by the opening and closing of the field around a blob. As one might imagine, the fact that the blobs are moving through a field of varying magnitude means that there will be a whole spectrum of waves set up in the atmosphere, dependent on position and time. The frequency of the oscillation is now determined by the blob size l and the local Alfvén speed (if we neglect the speed of sound in the magnetosphere and take $v = v_A$)

$$\Omega = kv_A \sim 2\pi v_A/l. \tag{25}$$

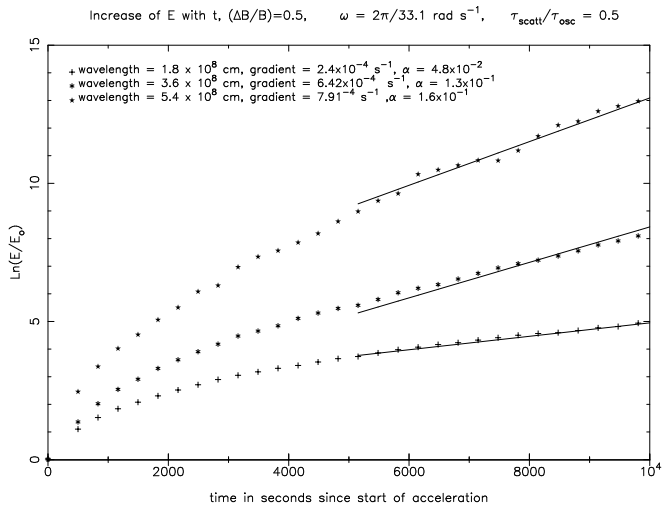

Fig. 4. The increase of energy with time of particles accelerated by travelling magnetic compressions.

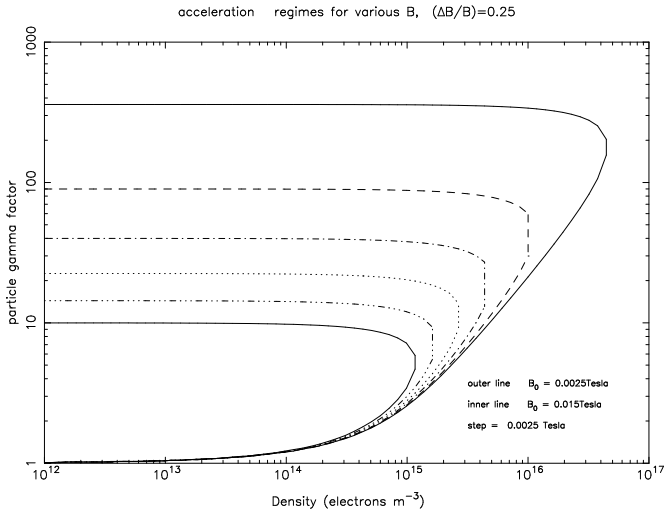

Fig. 5. Allowed acceleration regimes for τ_{scatt}/τ_{osc} = 1 and various field strengths (0.0025 – 0.015 T). A net acceleration will occur in the regions inside the curves.

However to keep things simple we shall give here values of the efficiency of acceleration in the atmosphere at the spin frequency ω but at a number of values of the parallel wave number $k_\parallel$ corresponding effectively to a number of values of Alfvén speed, which can be associated with regions of particular density at a particular position.

We model the field oscillation as a travelling wave of form

$$B(z,t) = B_o(1 + \epsilon(\cos(\omega t - k_\parallel z))), \tag{26}$$

where ϵ determines the amplitude of the field oscillation. Since the wave is travelling the effective oscillation time (the time which elapses between a particle meeting field compressions) is Doppler shifted and depends not only on the oscillation frequency but also on the particle velocity along the field. In this case we do not obtain a linear relationship at low energies. As particle velocity increases towards the speed of light, the relationship tends to a linear one. By comparing Figs. 2 and 4 it can be seen that at low energies acceleration by travelling waves can be more efficient than that by standing waves, but that the efficiency decreases as the particles become relativistic. Long wavelength oscillations are more efficient accelerators than short wavelength oscillations. The efficiency eventually tends to that of standing (infinite wavelength) oscillations.

We now turn our attention to the energy losses of the particles which have to be overcome by the acceleration.

5. Energy losses

An energy increase can only occur and be sustained if acceleration by magnetic pumping energises the system faster than energy is lost. Whilst they are accelerating, electrons can also lose energy by synchrotron losses, Coulomb losses or plasma instabilities of the loss-cone type. This will occur only in restricted regimes of background particle density, field strength and injected particle energy. In addition, the accelerated particles must be prevented in some way from leaving the magnetosphere so that there are sufficient left to account for a flare. We shall assume that plasma instabilities scatter the particles without absorbing much of their energy.

5.1. Coulomb and synchrotron losses

To find the allowed regimes for particle acceleration we solve the equation $\dot{\gamma}_{bet,av} + \dot{\gamma}_{synch} + \dot{\gamma}_{Coul} > 0$ for various cases of τ_{scatt}/τ_{osc} and initial magnetic fields. The synchrotron and Coulomb losses for electrons are given by (e.g. Leach & Petrosian 1981)

$$\dot{\gamma}_{synch} = -\frac{8\pi}{3m_e c} r_o^2 \left(\frac{B^2}{\mu_o}\right) \gamma^2 \beta^2 (1-\mu^2) \tag{27}$$

and

$$\dot{\gamma}_{Coul} = -\frac{4\pi n c r_o^2 \Lambda}{\beta}, \tag{28}$$

where $r_0 = e^2(4\pi\epsilon_0 mc^2)^{-1}$ is the classical electron radius, Λ the Coulomb logarithm, and n the background electron density. We arrive at a series of curves in (n,γ) space plotted here in Fig. 5. In this figure, acceleration can take place in the regions above and to the left of the curves.

A critical region is around the energy with which the particles are injected onto the field lines. It must be possible for the particles to begin accelerating right away via the magnetic pumping effect, otherwise we are forced to invoke a first step acceleration mechanism to take them up to some critical threshold energy, at which magnetic pumping can proceed. To examine this question we look at the low energy end of Fig. 5. If we

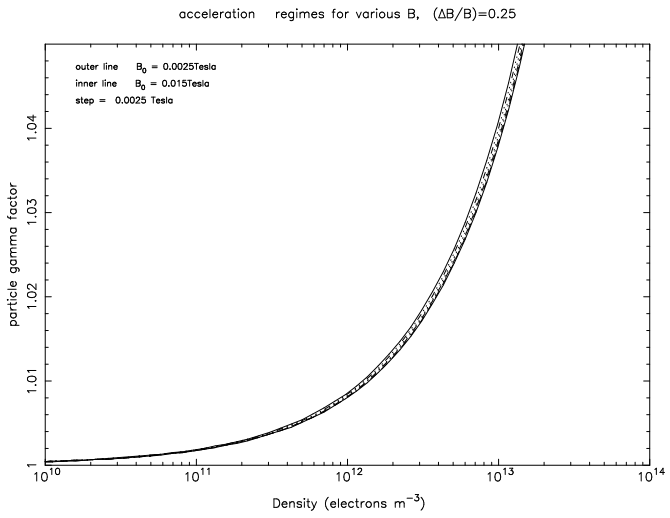

Fig. 6. The low energy end of Fig. 5.

assume that the accreting gas consists of fully ionised hydrogen with components in thermal equilibrium, then the thermal energy of electron and proton components is equal, i.e.,

$$\frac{1}{2}m_p v_p^2 = \frac{3}{2}kT = \frac{1}{2}m_e v_e^2. \tag{29}$$

If we further assume that the thermal energy of the gas derives from the infall energy, which is dominated by the more massive proton component, then

$$v_p^2 = \frac{2GM}{r} = \frac{m_e}{m_p}v_e^2. \tag{30}$$

At a radius of $5\cdot10^8$ m for example, the electron thermal velocity in the blob is $3\cdot10^7$ m s^{-1}, so the minimum energy it will have as it attaches to the field is then $\gamma - 1 = 5\cdot10^{-3}$. It is a minimum energy since by virtue of the rapid rotation of the white dwarf, the velocity of a 'pickup' electron in the frame of the moving magnetic field may be higher, depending on the radius at which it attaches.

So in regions of density of $\lesssim 6\cdot10^{11}$ particles m^{-3} betatron acceleration (assuming $\Delta B/B = 0.25$) of free-falling material may take place. Of course if they have a higher energy, particles may continue to accelerate in higher densities.

5.2. Particle losses and trapping.

If particles are to be accelerated by magnetic pumping, they must be maintained in the magnetosphere. Depending on factors such as the particle energy, pitch-angle and position in the magnetosphere, a particle will either precipitate onto the poles (due to synchrotron losses and Coulomb collisions) or be kept in the atmosphere by the magnetic mirror force (due to the converging magnetic field). The competition between energy loss and gain processes (as a function of density, field etc) determines the region where particles lose more energy than they gain, as described in the above section, whilst the magnetic field convergence and the particle energy and pitch-angle determine which particles will enter this region. Let the position r_{pr} be the position on a given field line at which losses dominate energy gains and particles precipitate out. Only a fraction of the particles will ever reach this critical position, and the loss-cone – the region in pitch-angle space encompassing all particles which will ultimately precipitate – at position r has a half-angle ψ defined by

$$\sin^2\psi(r) = \frac{B(r)}{B(r_{pr})}. \tag{31}$$

For magnetic pumping to work efficiently we must be in a regime of efficient scattering, which puts us in the strong diffusion limit. In this limit the loss-cone is always approximately full, with particles being scattered in and out continuously. The escape timescale is then $\tau_{esc} = \tau_{exit}/F$ where τ_{exit} is the time taken to diffuse along the loop, and F is the fraction of solid angle contained in the loss-cone. In a scattering medium this is the time taken to random walk across the structure,

$$\tau_{exit} = \frac{L^2}{2D_{zz}}, \tag{32}$$

where L is the length of the structure which the electrons have to cross, and $D_{zz} = v^2/6D_{\mu\mu}$ is the spatial diffusion coefficient. For small loss-cones, $F = \psi^2/2$. Taking an optimum value for $D_{\mu\mu} = 1/\tau_{osc} = 1/P_{wd}$ and using $v \sim c$ we get

$$\tau_{esc} = \frac{L^2}{5\cdot10^{17}\psi^2}\ \text{s}. \tag{33}$$

We see from Fig. 5 that synchrotron losses limit the maximum Lorentz factor. To derive the conditions on the loops in which particles can be accelerated up to a chosen Lorentz factor we determine the maximum field B_{max} allowed from Fig. 5 for that value of the Lorentz factor, and the corresponding acceleration time. This field value is then identified with that at the mirror point r_{pr}. Equation (33) together with (31) and the requirement that the trapping time exceeds the acceleration time then lead to the (conservative) condition

$$\frac{L^2 B_{max}(r_{pr})}{5\cdot10^{17}B(R_0)} > \tau_{acc}, \tag{34}$$

which for the determined values of B_{max} and τ_{acc} identifies the smallest loop in the given field structure where acceleration up to the required energy can take place. For a dipolar structure the loop half-length is $L = 1.38R_0$, where R_0 is the radial distance from the stellar centre.

Let us apply this to particles of $\gamma \sim 100$. The maximum field strength (Fig. 5) is 0.005 T. The acceleration time is $1.5\cdot10^4$ s for $\Delta B/B = 0.25$ and 10^3 s for $\Delta B/B = 1$. Particles initially attaching to the field at radii greater than, respectively, $240R_{wd}$ ($B = 7.28\cdot10^{-6}$ T, $\psi = 1.46\cdot10^{-3}$) and $140R_{wd}$ ($B = 3.70\cdot10^{-5}$ T, $\psi = 7.40\cdot10^{-3}$) will not precipitate in less than the acceleration time.

6. Emission from AE Aquarii

Having outlined the acceleration mechanism and found the regimes in which it may operate, we now proceeed to see whether it can explain the radio emission which we observe in AE Aqr.

6.1. Quiescent radio emission

Can acceleration by magnetic compressions power the quiescent radio emission from AE Aqr? Since the radio spectrum is observed to increase with frequency up to at least ν = 394 GHz (Abada-Simon et al. 1995a) we shall assume that the majority of quiescent emission is output around this frequency. Assuming that the emission is synchrotron radiation, the characteristic individual particle energy is (Pacholczyk 1970)

$$E = 8.4 \cdot 10^{-19} B^{-1/2} \nu^{1/2} \mathrm{J} = 5.3 \cdot 10^{-13} B^{-1/2} \mathrm{J}, \quad (35)$$

or $\gamma = 6.42 B^{-1/2}$ (91 in a $5 \cdot 10^{-3}$ T field). The particles would have to be accelerated to this energy and then kept there by pumping, balancing out with synchrotron and Coulomb energy losses in a steady-state situation. The loss of energy in synchrotron radiation of each particle is given by Eq. (27), and inserting the value for the Lorentz factors of emitting particles gives the total synchrotron power for a volume V of particles at density n_e,

$$P_{synch} = 4.36 \cdot 10^{-13} B \left(1 - \frac{B}{41.2}\right) n_e V \ \mathrm{W} \quad (36)$$

(integrating over solid angle, assuming an isotropic distribution and an optically thin cloud). From Fig. 5 we see that the magnetic field must be $\lesssim 5 \cdot 10^{-3}$ T for a net acceleration to appropriate energy to take place (determined by $\gamma = 6.42 B^{-1/2}$). Therefore we need $\sim 5 \cdot 10^{34}$ emitting electrons to explain the quiescent emission at 10^{20} W. Acceleration can occur (giving a sustainable emission of synchrotron radiation) in cold plasma densities $n \lesssim 6 \cdot 10^{11} \mathrm{m}^{-3}$. Also, for a steady source the particle energy density should remain smaller than the energy density of the magnetic field, $n_e \gamma m_e c^2 < B^2 (2\mu_0)^{-1}$, which leads to an upper limit on the fast particle density of $n_e \lesssim 1.34 \cdot 10^{12}$ m^{-3} (for a Lorentz factor γ = 91 and a field strength B = 0.005 T). Then the source volume is at least $V \gtrsim 8.3 \cdot 10^{22}$ m^3. If the white dwarf surface field at the poles is 100 T, this corresponds to a spherical shell of minimum thickness 10^5 m at the distance at which the field equals $5 \cdot 10^{-3}$ T ($\sim 27\ R_{wd} = 2.7 \cdot 10^8$ m). As detailed in the previous section precipitation losses increase this distance further.

It therefore seems possible that the quiescent radio emission can be explained by continuous energisation of the particles by the large-scale standing field oscillations.

6.2. Flare radio emission

To produce flares, we would envisage a situation in which enough particles are trapped on the field lines of the white dwarf and subsequently take part in the acceleration process. As the energy density in fast particles becomes too large with respect to that in the field, a MHD instability sets in and a magnetic cloud containing accelerated particles is expelled.

The number of energetic particles that may be stored in the white dwarf magnetosphere depends both on the magnetic field geometry and on where the energetic particles are produced. If they are deposited within a narrow flux tube a ballooning instability is likely, leading to an outward expansion of the flux tube releasing a cloud of energetic particles. To find the conditions for this it is necessary to specify the size and location of the region where the particles are deposited.

If the energy of stored particles E_p, deposited at a radius R_e, is comparable to the magnetic energy $\Delta E_B(R_e)$ required to open the field beyond R_e, the closed field lines will open up releasing them. Approximating the open field B_{open} by a uniform radial field which reverses direction at a current sheet in the equatorial plane, with a flux given by a dipole magnetic flux at R_e, we have $B_{open} = \pm(\pi B_{wd} R_{wd}^3 / R_e)(1/2\pi r^2)$. Neglecting the change in magnetic energy for $r < R_e$, the condition for releasing the stored particles is, $W_p \geq \Delta E_B(R_e) \approx \pi/3\ R_{wd}^3\ (B_{wd}^2/\mu_0)(R_{wd}/R_e)^3$. If we take B_{wd} = 100T, $R_{wd} = 10^7$m as canonical values for the white dwarf magnetic field and radius this maximum stored energy is $E_p \sim 4.2 \cdot 10^{30} (R_e/R_{wd})^{-3}$ J. For example if the minimum radius at which energisation dominates over losses is $R_e = 30 R_{wd}$, we expect the stored particles to be released if their energy exceeds $1.6 \cdot 10^{27}$ J.

Once the cloud of trapped particles has been released from the magnetosphere much of the particle energy will go towards expanding the plasmoid. The individual particle energy will decrease as $E \propto r_s^{-1}$ as the source radius r_s increases. For an observed luminosity of 10^{21} W, a source size r_s, and a bandwidth $\Delta\nu \sim \nu$ the brightness temperature at 400 GHz is given by

$$K_B T_b \sim 1.11 \cdot 10^6 r_{s7}^{-2} \ \mathrm{eV}, \quad (37)$$

and the source is initially optically thin for $\gamma - 1 > 2 r_{s7}^{-2}$. Therefore at this frequency the brightness temperature decreases as the plasmoid expands. However at lower frequencies, taking into account the observed average positive slope of the spectrum (index ~ 0.5), the brightness temperature increases $T_b \propto \nu^{-1.5}$ and the source is initially optically thick. In fact the observed positive frequency slope of the quiescent average radio flux and the transition from optically thick to thin emission in a flare (Bastian et al. 1988) can be understood if a constant number of electrons are gradually accelerated to larger and larger energies within the same loop structure until it bursts open.

Finally, note that the emission at the time of the outbreak of the plasmoid is rather efficient as the synchrotron loss-time equals the acceleration time.

6.3. Hard X-ray emission by trapped and precipitating particles

To determine if trapped particles would emit observable quantities of X-rays we calculate the hard X-ray luminosity from:

$$L = \frac{64\pi}{3}\sqrt{\frac{1}{2}}\frac{e^6}{m_e c^2 h(4\pi\epsilon_o)^3}\sqrt{\frac{kT}{m_e c^2}}(\sum_z n_e Z^2 n_z V), \qquad (38)$$

where L is the hard X-ray luminosity, T is the temperature of the emitting plasma, n_e and n_z are the electron and ion densities with electric charge Z, and V is the volume of the emitting plasma. The term in brackets is the so-called emission measure (EM) which can be simplified as n_e^2 V. The above equation can therefore be re-written as:

$$L = 1.38 \cdot 10^{-40}\sqrt{T} n_e^2 V \text{ W}. \qquad (39)$$

From §5.1 and §6.1 we take $n_e \lesssim 5 \cdot 10^{12}$ m^{-3}, V $\gtrsim 10^{22}$ m^3, v_e (the thermal electron velocity) =$3 \cdot 10^7$ m s^{-1} (which implies an electron temperature of $\sim 10^7$ K) and find $L_{hard} \gtrsim 10^{11}$ W. This figure is many orders of magnitude less than the observed hard X-ray flux, $L_{hard} \sim 10^{24}$ W (Eracleous et al. 1991). We conclude that the particles energised by magnetic pumping would not contribute a significant proportion to the observed hard X-ray flux.

If we assume that a small fraction of these energised particles (say 1%) can escape from the magnetosphere (see §4) and generate thick target emission near the stellar surface, the hard X-ray emission from these particles would be $L \sim 0.01 N\gamma m_e c^2/\tau_{flare} \sim 2.2 \cdot 10^{18}$ W for $N = 10^{35}$, $\gamma = 100$, and $\tau_{flare} = 1$ hour. If the hard X-rays are generated from tall accretion curtains of the sort described by Eracleous et al (1995), it is clear that the emission from the accelerated particles would not contribute a significant amount to the overall X-ray flux and are not the origin of the X-rays seen in AE Aqr (Clayton & Osborne 1995).

7. Discussion

To put our results into perspective we briefly discuss the injection of the particles into the accelerator and other acceleration mechanisms expected to occur in AE Aqr.

The maximum number of radiating electrons is $10^{36} - 10^{37}$. Assuming that they have to be refreshed every hour (the flare timescale) an equivalent hydrogen mass accretion rate of $4.6 \cdot 10^5$ kg/s = $7 \cdot 10^{-18}$ M$_\odot$/ yr has to be supplied for, which is a fraction 10^{-6} of the nominal accretion rate. Two sources of gas injection are the wind from the secondary and Roche lobe overflow from the secondary in the form of clumps of matter.

Considering Roche lobe overflow first, gas clumps falling towards the white dwarf quickly reach supersonic speeds. Assuming that the motion is supersonic (or super-alfvénic) with respect to both the magnetosphere and the internal velocity of sound in the blob, a system of two shocks forms, separated by a contact discontinuity. At the outer shock the incoming magnetospheric plasma is compressed and heated. The inner shock pressurises the gas blob and vanishes when there has been enough time for the shock to reach the blob center. The details depend on the blob density and dimensions as they determine the cooling rate. In any case Kelvin-Helmholtz and Rayleigh-Taylor instabilities are expected to develop along the contact discontinuity toward the wake, gradually stripping the gas blob. Note that the short-periodic, dramatic increase of ambient magnetic field pressure (with a factor 4 for a perpendicular rotator) shocks the gas blobs continuously. Ablation turns the stream of gas blobs into a spray (cf. Wynn et al. 1995). Ultimately the ambient field penetrates the fragments or part of them (Arons & Lea 1980) and magnetic pumping starts acting on the plasma. This process is enhanced by the so-called pickup process (see below) of initially neutral gas atoms escaping from the blob surface into the magnetosphere.

The second source of plasma is the stellar wind of the companion. If the stellar mass loss rate is comparable to the, extremely weak, solar one ($2 \cdot 10^{-14}$ M$_\odot$/yr) a fraction $4 \cdot 10^{-4}$ of the particles have to get injected into the accelerator. Of course strong magnetic activity (see below) in the corona of the secondary enhances the mass loss rate in the stellar wind. Moreover erupting stellar prominences, in particular unstable prominences in the reversed gravity field above the inner Lagrangian point could enhance the mass transfer. Such 'prominences' with estimated densities of 10^{18} m^{-3} can act as long-term injectors of particles in dwarf novae (Steeghs et al. 1996).

Finally, in the fast rotating magnetosphere cool matter can be held-up against gravity at preferred locations (Steeghs 1996).

We now briefly turn to acceleration processes other than magnetic pumping.

7.1. Pickup acceleration

Neutral gas atoms evaporating from the infalling blobs can penetrate the white dwarf magnetosphere. As soon as the atoms get ionized their charged constituents become trapped onto the white dwarf magnetic field with particle speeds at least equal to the differential speed of the blob and the magnetosphere $\beta = v/c = \omega_{wd} r/c \approx 6.4 \cdot 10^{-3} R_0/R_{wd}$. For instance at a hundred white dwarf radii the kinetic pickup energy of an electron would be 150 keV, and 300 MeV for a proton. The pickup process can be enhanced by microinstabilities driven by the relative motion between the new ions and the background plasma. This occurs in the critical ionisation velocity mechanism. The theory (Raadu 1978) invokes the modified two stream instability which accounts for the observed electron energisation parallel to the magnetic field (Danielsson & Brenning 1975) with energies comparable to the kinetic pickup energy of the ions. Thus the pickup process can produce electrons with energies much greater than their pickup energies. Clearly, the pickup process can be a very important injection process for magnetic pumping.

7.2. Transit-time damping

For small-amplitude wave-like perturbations transit-time magnetic pumping requires a Čerenkov resonance to be fulfilled

$$\omega - k_\parallel v_\parallel = 0, \qquad (40)$$

where $(\omega(\boldsymbol{k}), \boldsymbol{k})$ are the wave frequency and the wave vector, respectively, and the relevant components are taken parallel to the ambient magnetic field. Further only compressional magnetic waves –the fast and the slow mode – contribute (Achterberg 1981). Equation (40) is familiar from Landau damping when the wave has a longitudinal electric field component. As has been shown by Stix (1992) transit-time pumping is the magnetic analogue of Landau damping. Actually both effects interfere and should be taken into account to determine the rate of transfer of energy from waves to particles. For the nearly perpendicular fast magnetosonic wave, however, the electric field component along the magnetic field is much smaller than the electric field component transverse to both the magnetic field and the wave vector and Landau damping can be neglected compared to transit-time damping. For an isothermal plasma primarily electrons rather than ions are heated by collisionless transit-time damping of fast magnetosonic waves. Transit-time damping could play an important role in AE Aqr, if only to preheat electrons (and ions). In particular a non-linear version of transit-time damping is expected to operate on those field lines where the bounce time of a particle equals the oscillation time which in our case is the rotation period of the white dwarf. From Eq. (15) it follows that loops with shell parameter

$$\frac{R_0}{R_{wd}} = 248\frac{\beta}{f_1(\theta_0)} \sim (180 - 335)\beta \tag{41}$$

will be heated by this process. We conclude that a future investigation of transit-time damping in AE Aqr for large amplitudes is needed.

7.3. Resonant heating

Another process of interest, which has been investigated in the context of heating the solar corona (Kuperus et al. 1981, Goedbloed & Halberstadt 1994, Poedts & Boynton 1996), is resonant heating by Alfvén waves. The mechanism is based on the resonance between the Alfvén propagation time along a particular field line of length l, which is anchored at its footpoints in the star, and the frequency of an MHD wave ω impinging on the inhomogeneous magnetic loop structure

$$\omega = \frac{\pi Z v_A}{l}, \tag{42}$$

with integer Z. In the layer of field lines satisfying this equation for given ω, a standing kinetic Alfvén wave can be excited to a large amplitude. Radial inhomogeneity then leads to phase mixing and the development of large gradients. The incoming Poynting flux of the MHD wave is then efficiently tapped by strong dissipation either by viscous damping and Ohmic heating, or collisionless damping. Taking the speed of light as an upper limit to the Alfvén parameter resonant heating by MHD waves at the spin period is found to be important for dipolar loops with shell parameter

$$\frac{R_0}{R_{wd}} \leq 57. \tag{43}$$

Again this is an interesting process requiring further study.

7.4. Magnetic flares and reconnection

As we have seen, magnetic pumping can lead to eruptions. These can be called magnetic flares as they originate from a large-scale instability of an MHD structure. It is important, however, to realize that our flares are pressure-driven by the high energy particles stored in the magnetic fields. This is at variance with solar flares which are considered to be driven by the evolving magnetic field of a low-beta structure (Kuijpers 1992, $\beta_{gas} = 2\mu_0 p_{gas}/B^2$ is the ratio of gas pressure to magnetic field pressure). We merely point out here that such 'classical' flares could occur as well in AE Aqr and lead to particle acceleration. Two obvious cases present themselves: firstly, reconnection between coronal magnetic fields of the companion and of the white dwarf may lead to coronal current systems (Lamb et al. 1983) and subsequent explosions. The formation of such flaring structures would primarily occur where the fields of the companion and white dwarf are comparable. For the above dipolar field of the white dwarf and a surface field of the companion at the inner Lagrangian point ($1.1 \cdot 10^9$ m from the white dwarf) of 0.3 T with a dipolar scale height of $2 \cdot 10^7$ m the magnetic fields are comparable ($1.6 \cdot 10^{-4}$ T) at the midpoint between the stars (about $R_0/R_{wd} = 85$ from the white dwarf). The total energy which could be stored in such a huge weak field structure is of the order of the potential energy, $W_M \sim B^2R^3/2\mu_0 = 6 \cdot 10^{24}$ J. Of course this estimate implies reconnection at the speed of light, assumes that the surface of the companion is covered with strong fields, and moreover neglects the complicating shock structure which engulfs the companion. Therefore, it seems unlikely that such large-scale reconnections between the fields of the companion and white dwarf are sufficiently powerful to cause the observed radio outbursts. Secondly and more promising, the ambient white dwarf field can be distorted (and reconnect) by infalling blobs in a manner such as described by Aly & Kuijpers (1990).

Finally other acceleration processes can be important such as shock acceleration by bullets (Jones et al. 1994), magnetic field aligned electric fields in AC or DC circuits (Raadu 1989), and modulational instabilities of magnetosonic waves (Bingham 1995 private communication), and it would be important to have observations which discriminate between these (such as TeV γ-rays, De Jager et al. 1994, Meintjes et al. 1994).

7.5. Flares on other magnetised binaries?

If our proposal that magnetic pumping creates plasmoids of cosmic rays in AE Aqr is correct, what are the predictions for other magnetic CVs and for X-ray binaries with neutron stars? Qualitatively, we expect that magnetic pumping is at work if the compact object is spinning fast, if its magnetic field is strong, and if the mass transfer rate is, on one hand large enough to tap the spin energy, and, on the other hand sufficiently small that low densities can be maintained in the magnetosphere required for magnetic pumping. In the case of white dwarfs, the magnetic field should not be too large because otherwise, as the observations show, the white dwarf becomes locked to the companion

and the spin rate adjusts to the orbital revolution rate. In the case of neutron stars the latter effect is not important because their magnetic moments are less than for white dwarfs. To get some idea of the permitted initial density of non-relativistic particles we put $\dot{\gamma}_{bet,av} + \dot{\gamma}_{Coul} > 0$ to obtain (see Eqs. (19) and (28))

$$n < 1.7 \cdot 10^{16} \beta^3 P_*^{-1} \text{ m}^{-3}, \tag{44}$$

for a star of period P_* in seconds, $\Delta B/B = 0.25$, and $\Lambda = 20$. Transforming this number into an effective mass accretion rate we find $\dot{M}_{eff} \sim 4\pi R_0^2 n m_i v \sim 1.05 \cdot 10^{11} P_*^{-1}$ kg/s, with $R_0 = 10^8$ m, and $\beta = 0.1$. This number remains many orders of magnitude below the critical mass accretion rate even for the fastest spinning neutron star. We expect this effective mass accretion rate to depend monotonically on the real mass accretion rate onto the compact star, and to set an upper limit to it if magnetic pumping operates. Further the pumping process and the loop eruption require the particles to be trapped and therefore located inside the light cylinder $r_{lc} = 4.8 \cdot 10^7 P$ m. This sets a lower limit to the spin period. Also note in this respect that a trapped cloud of fast electrons near a neutron star is only observable as a synchrotron source at radio frequencies if it is large enough ($\gtrsim 10^8$ m, Kuijpers 1989). Finally from $\dot{\gamma}_{bet,av} + \dot{\gamma}_{synch} = 0$ we obtain an estimate of the characteristic equilibrium Lorentz factor (see Eqs. (19) and (27))

$$\gamma = 7.7 \cdot 10^{-2} P_*^{-1} B^{-2}, \tag{45}$$

for the same field oscillation amplitude as before. Note that B is the field strength in the source. We intend to elaborate these points in a future paper.

8. Conclusions

If the fast spinning white dwarf in AE Aqr has a surface field of 100 T magnetic pumping is a serious candidate for the particle acceleration needed to explain the observed radio outbursts. We have studied the various physical conditions that are required. The most efficient radiator of strong magnetic oscillations is a stream of gas blobs from the secondary into the magnetosphere of the white dwarf. Further an important ingredient for magnetic pumping to work is to put a sufficient amount of dilute plasma onto the magnetic field lines, and to keep the particles trapped long enough for the accelerator to work. To have efficient pumping a scattering process is required such that the pitch angle scattering time matches the oscillation time of the field. For simplicity we have limited ourselves to oscillations at the spin period, although perturbations exist also at higher frequencies. We have just assumed that a suitable plasma instability takes care of the scattering, and more work is needed to demonstrate that such an instability occurs. Note that plasma instabilities caused by loss-cone distributions can also lead to radio emission. However, a clear signature of a coherent emission process is lacking in the majority of the radio observations in AE Aqr. On particular magnetic field lines the MHD oscillations lead to particle acceleration also by the processes of transit-time damping and resonant heating, and these processes deserve further study. The injection energy appears to be no problem, both because of the initial particle energy in the gravitational well of the white dwarf and because of the rapid rotation which gives a high initial pickup energy to ionized atoms. The accelerated particles are not the origin of the X-rays seen in AE Aqr. Finally our proposal of magnetic pumping of a particle trap anchored in the white dwarf and its subsequent expulsion seems to explain the pertinent radio observations of AE Aqr.

Acknowledgements. Part of this work was performed under EC-twinning contract No. SCI*-CT91-0727 on Coherent Radiation and Particle Acceleration in Magnetized Plasmas, and CEC HCM Network ERBCHRXCT 940604 on Energetic Particles in Astrophysical and Space Plasmas. M.A.-S. and G.R. gratefully acknowledge postdoctoral institutional fellowships from the EC on Astrophysics of Accretion and Winds near Compact Objects under contract number ERBCHBGCT 93-0998. D.S. gratefully acknowledges support from the Erasmus programm ICP-94-B-3047/13 for a visit to St. Andrews. It is a pleasure to thank Bram Achterberg, Bob Bingham, Yves Gallant and Michel Tagger for their comments.

References

Abada-Simon, M, Bastian, T.S., Bookbinder, J.A., et al.: 1995a, in IAU Coll. 151, Flares and Flashes, eds. J. Greiner, H.W. Duerbeck, R.E. Gershberg, Lecture Notes in Physics, 454, Springer

Abada-Simon, M, Bastian, T.S., Horne, K., Robinson, E.L., Bookbinder, J.A.: 1995b, in Cape Workshop on Magnetic Cataclysmic Variables, eds. D.A.H. Buckley and B. Warner, ASP Conference Series No. 85, San Francisco, p. 355

Abada-Simon, M., Lecacheux, A., Bastian, T.S., Bookbinder, J.A., Dulk, G.A.: 1993, ApJ 406, 692

Achterberg, A.: 1981, A&A 97, 259

Achterberg, A., Krülls, W.: 1992, A&A 265, L13

Alfvén, H.: 1954, Tellus 6, 232

Alfvén, H., Fälthammar, C.-G.: 1963, Cosmical Electrodynamics, Clarendon Press, Oxford, Ch. 2

Aly, J.J., Kuijpers, J.: 1990, A&A 227, 473

Arons, J., Lea, S.M.: 1980, ApJ 235, 1016

Bailey, J.: 1981, MNRAS 197, 31

Barnett, A., Olbert, S.: 1986, JGR 91, 10117

Bastian, T.S., Dulk, G.A., Chanmugan, G.: 1988, ApJ 324, 431

Berger, J.M., Newcomb, W.A., Dawson, J.M., et al.: 1958, Phys. Fluids 1, 301

Clayton, K. L., Osborne, J. P.: 1995, in Cape Workshop on Magnetic Cataclysmic Variables, eds. D.A.H. Buckley and B. Warner, ASP Conference Series No. 85, San Francisco, p. 379

Cropper, M.: 1990, Space Sci Rev 54, 195

Danielsson, L., Brenning, N.: 1975, Phys. Fluids 18, 661

De Jager, O.C.: 1994, ApJ Suppl Series 90, 775

De Jager, O.C., Meintjes, P.J.: 1993, A&A 268, L1

De Jager, O.C., Meintjes, P.J., O'Donoghue, D., Robinson, E.L.: 1994, MNRAS 267, 577

Eracleous, M., Halpern, J., Patterson, J.: 1991, ApJ 382, 290

Eracleous, M., Horne, K., Robinson, E.L., et al.: 1994, ApJ 433, 313

Eracleous, M., Horne, K., Osborne, J. P., Clayton, K. L.: 1995, in Cape Workshop on Magnetic Cataclysmic Variables, eds. D.A.H. Buckley and B. Warner, ASP Conference Series No. 85, San Francisco, p. 392

Fermi, E.: 1954, ApJ 119, 1
Fletcher, L: 1995, A&A 303, L9
Fletcher,L., Brown, J.C.: 1995, A&A 294, 260
Frank, J., King, A., Raine, D.: 1992, Accretion Power in Astrophysics, Cambridge Univ. Press, p. 271
Goedbloed, J., Halberstadt, G.: 1994, A&A 286, 275
Goldston, R.J., Rutherford, P.H.: 1995, Introduction to Plasma Physics, Inst. of Phys. Publ., Bristol, Ch. 4
Hjellming, R.M., Penninx, W.: 1991, in Particle Acceleration near Accreting Compact Objects, eds. J. van Paradijs, M. van der Klis and A. Achterberg, Kon. Ned. Academie van Wetensch., Verh., Afd. Natuurkunde, Eerste Reeks, deel 35, North-Holland, Amsterdam, p. 109
Horne, K., Eracleous, M.: 1995, in Cape Workshop on Magnetic Cataclysmic Variables, eds. D.A.H. Buckley and B. Warner, ASP Conference Series No. 85, San Francisco, p. 244
Jones, T.W., Kang, H., Tregillis, I.L.: 1994, ApJ 432, 194
Kirk, J.: 1995, in Plasma Astrophysics, eds. A.O.Benz and T.J.-L. Courvoisier, Saas-Fee Advanced Course 24, Springer-Verlag, Berlin, p. 225
Kopp, A.: 1996, JGR 101, 24,943
Krülls, W.M, Achterberg, A.: 1994, A&A 286, 314
Kulsrud, R.M., Ferrari, A.: 1971, Astrophys. Space Sci. 12, 302
Kuijpers, J.: 1989, Solar Phys. 121, 163
Kuijpers, J.: 1992, in The Sun: A Laboratory for Astrophysics, eds. J.T. Schmelz and J.C. Brown, Kluwer Acad. Publ., Dordrecht, p. 535
Kuperus, M., Ionson, J.A., Spicer, D.S.: 1981, ARAA 19, 7
Lamb, D.Q.: 1988, in Polarized Radiation of Circumstellar Origin, eds. G.V. Coyne et al., Vatican Observatory (Vatican City State), p. 151
Lamb, D.Q., Patterson, J.: 1983, in IAU Coll. 72, eds. M. Livio and G. Shaviv, Reidel Publ. Cy., Dordrecht, p. 229
Lamb, F.K., Aly, J.-J., Cook, M.C., Lamb, D.Q.: 1983, ApJ 274, L71
Leach, C.F, Petrosian, V.: 1981, ApJ 251, 781
Lüttgen, A., Neubauer, F.M.: 1994, JGR 99, 23,349
Lyons, L.R., Williams, D.J.: 1984, Quantitative Aspects of Magnetospheric Physics, D. Reidel Publ. Cy., Ch. 2
MacKinnon, A.L., Craig, I.J.D.: 1991, A&A 251, 693
Meintjes, P.J., De Jager, O.C., Raubenheimer, B.C., Nel, H.I., et al.: 1994, ApJ 434, 292
Melrose, D.B.: 1980, in Plasma Astrophysics, Gordon and Breach, Vol. II, p. 73
Möbius, E.: 1994, ApJ Suppl. Ser. 90, 521
Mouchet, M., Casares, J., Harlaftis, E.T., et al.: 1995, in Cape Workshop on Magnetic Cataclysmic Variables, eds. D.A.H. Buckley and B. Warner, ASP Conference Series No. 85, San Francisco, p. 359
Nelson, R.F., Spencer, R.E.: 1988 MNRAS 234, 1105
Pacholczyk, A.G.: 1970, in Radio Astrophysics, Nonthermal Processes in Galactic and Extragalactic Sources, ed. W.H. Freeman and Company, San Francisco, p. 68
Patterson, J., 1994: PASP, 106, 209
Poedts, S., Boynton, G.C.: 1996, A&A 306, 610
Raadu, M.A.: 1978, Astrophys. Space Sci. 55, 125
Raadu, M.A.: 1989, Phys. Reports 178, 25
Reinsch, K., Beuermann, K., Hanusch, H., Thomas, H.C.: 1995, in Cape Workshop on Magnetic Cataclysmic Variables, eds. D.A.H. Buckley and B. Warner, ASP Conference Series No. 85, San Francisco, p. 115
Roederer, J.G.: 1970, Dynamics of Geomagnetically Trapped Radiation, Springer-Verlag, Berlin, Ch. 1
Scheurwater, R., Kuijpers, J.: 1988, A&A 190, 178
Schlüter, A.: 1957, Z. Naturforschg. 12a, 822
Spitzer, L.: 1962, Physics of Fully Ionized Gases, Intersc. Publ., John Wiley & Sons, New York, Ch. 1.4
Steeghs, D.: 1996, Graduation Thesis, Utrecht University
Steeghs, D., Horne, K., Marsh, T., Donati, J.F.: 1996, MNRAS 281, 626
Stix, T.H.: 1992, Waves in Plasmas, American Institute of Physics, New York
Stockman, H. S., Schmidt, G. D., Berimann, G., et al.: 1992, ApJ 401, 628
Swann, W.F.G.: 1933, Phys. Rev. 43, 217
Welsh, W.F., Horne, K., Gomer, R.: 1994, MNRAS 257, 649
Welsh, W.F., Horne, K., Oke, R.: 1993, ApJ 406, 229
Wynn, G.A., King, A.R., Horne, K.D.: 1995, in Cape Workshop on Magnetic Cataclysmic Variables, eds. D.A.H. Buckley and B. Warner, ASP Conference Series No. 85, San Francisco, p. 196
Wynn, G.A., King, A.R., Horne, K.: 1996, MNRAS, in preparation

This article was processed by the author using Springer-Verlag LaTeX A&A style file *L-AA* version 3.